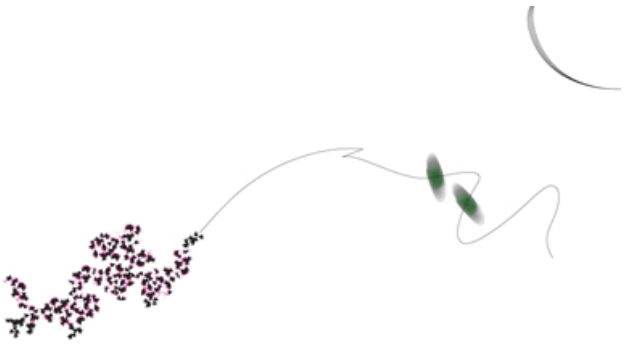

University of Twente

Bachelor Assignment

Performance of platinized TiO_2 on organic dye degradation coupled with H_2 production

Author:
Nikodem Bienia, s1195786

Supervisor:
Prof. Dr. Guido Mul
Joana Sobral Romao

External Member:
Dr. Ir. Mark Huijben

Advanced Technology

July 8, 2014

Abstract

A platinum loaded TiO_2 P25 catalyst was prepared by photodeposition procedure. Process related control mechanisms as stirring rate and UV intensity show high sensitivity with respect to noble metal deposition. The presence of platinum shows consistent minor improvements in photoactivity with different impacts for various organic compounds. Degradation is determined by measuring the absorption spectrum using UV spectrocscopy. Hydrogen evolution measurements were done with a gas chromatograph in combination with a thermal conductivity detector. The catalytic effect of platinum shows strong improvement in hydrogen production. In the absence of sacrificial agents electron-hole recombination dominates having a detrimental effect on the reduction of protons forming hydrogen. The combination of Methanol and formic acid (FA) with an organic contaminant (methyl orange (MO) /acid orange 7 (AO)) showed a big improvement in hydrogen production. The addition of organic compounds results in effects which depend on the pH of the solution. In the case of MO, acidic environments at pH levels of 2 result in nearly direct decolorization with an obvious mitigation of hydrogen production. At pH levels of 5 an improvement of hydrogen production can be observed which exceeds the production rate of systems without organic compounds which was demonstrated by using MO and methanol. For that case complete degradation was reach after approximately 25 minutes. It was successfully shown that degradation of pollutants in waste water can be coupled with hydrogen production with positive effect for one of the processes based on the pH of the system.

Contents

List of Figures

List of abbreviations

Symbol	Unit	Meaning
TiO_2	none	Titanium dioxide
$\hbar$	$m^2 kg\ s^{-1}$	Planck's constant = $6.626 \cdot 10^{-34}$
ν	s^{-1}	Frequency
e^-	none	Electron in the conduction band
h^+	none	Positive hole in the valence band
H^+	none	Proton (positively charged hydrogen atom)
H_2	none	Hydrogen molecule
O_2	none	Oxygen molecule
O_2^-	none	Superoxide ion
E_b	eV	Band gap
H_2O	none	Water
OH	none	Hydroxyl molecule
P	none	Pollutant
P^+	none	Oxidized pollutant
CB	none	Conduction band
VB	none	Valence band
M^{n+}	none	Positively charged metal
$M\downarrow$	none	Deposited metal
SED	none	Sacrificial electron donor
SED^+	none	Oxidized electron donor
A	none	Absorption
ϵ	$m^2\ mol^{-1}$	molar extinction coefficient
b	cm	path length
C	$mol\ L^{-1}$	Concentration
λ	nm	wavelength
d	nm	plane distance
θ	none	incident light angle
MeOH	none	Methanol
Pt	none	Platinum
H_2PtCl_6	none	Chloroplatinicacid
MO	none	Methyl orange
AO	none	Acid orange 7
FA	none	Formic acid
XRD	none	X-ray diffraction
H_2O_2	none	Hydrogen peroxide
BET	none	Brunauer-Emmett-Teller

Table 1: List of abbreviations

1 Introduction

1.1 Photocatalysis

1.1.1 Background

In recent years environmental problems got increased attention and much research is done to create green technology and find ways of waste disposal. One major concern is the access to clean water with rising demand by industry and population growth. Various chemical processes involve the use of water resulting in its contamination with byproducts which enter the water cycle. Many techniques to clean water focus on separation processes resulting in concentrating waste without eliminating it completely. Photocatalysis is a promising technology allowing to transform harmful waste into harmless endproducts as water, carbon dioxide and hydrogen [1].

1.1.2 Mechanisms of photocatalysis

In heterogeneous photocatalysis the electronic structure of the semiconductor catalyst plays a key role. Light with energy equal or higher than the band gap has the potential to promote electrons from the valence band (VB) to the conduction band (CB) leaving a positive hole in the VB [1]. This reaction is expressed in the following form:

$$\mathrm{TiO_2} \xrightarrow{\hbar\nu} \mathrm{e^-_{TiO_2}} + \mathrm{h^+_{TiO_2}} \tag{1.1}$$

The created electron-hole pair can recombine and release the excess energy in form of heat or photons. Simultaneously, charge can transfer from the bulk to the surface of the catalyst and react with adsorbed reactants, performing a reduction or oxidation reaction. For successful degradation an energy potential has to be overcome based on the reactant, meaning that the electron needs to have a more negative and the hole a more positive potential than required for reduction and oxidation, respectively [1]. The reactants have to be in either a gas or liquid phase [2]. Since the recombination of electron-hole pairs happens simultaneously with the charge transfer and the surface reaction only a fraction of the light is used for degradation which is known as the quantum efficiency of a photocatalyst. Long electron-pair lifetime and fast charge transfer increases the quantum efficiency [3]. Next to the degradation characteristics such as charge transfer, electron-pair lifetime, CB and VB potentials, the catalyst has to possess chemical stability such that it stays inert in environments exposing light and chemicals.

Several methods exist to enhance the catalytic functionality of the catalyst in form of chemical additives and noble metal loading. Chemical additives, also referred to as sacrificial agents, behave as electron donors or acceptors. This function allows to increase the catalyst's photoactivity by either accepting CB electrons, increasing the hydroxyl radical concentration which increases the oxidation rate of intermediates, or generation of other radicals with the potential to oxidize intermediates [4]. When placed in an acidic solution (pH $<$ 4.5) the catalyst will become positively charged posing an attraction force upon negatively charged compounds leading to a faster adsorption and thus, faster reaction kinetics [5]. Attraction repulsion interactions can be tuned by changing the pH of the solution which has an effect on the adsorption behavior of pollutants [6]. A second method for improved photocatalytic properties is to apply noble metal loadings with materials as Pt, Au or Pd. [1]. Noble metals have two main effects on the degradation of reactants, first they behave as electron

traps by creating a schottky barrier and thus, reduce the electron-hole recombination probability [7]. Second, they have a catalytic effect on reduction processes for compounds as hydrogen and oxygen by reducing the over potential and therefore, increasing the reaction kinetics [8]. A scheme of the photocatalytic process is displayed in Figure 1.1.

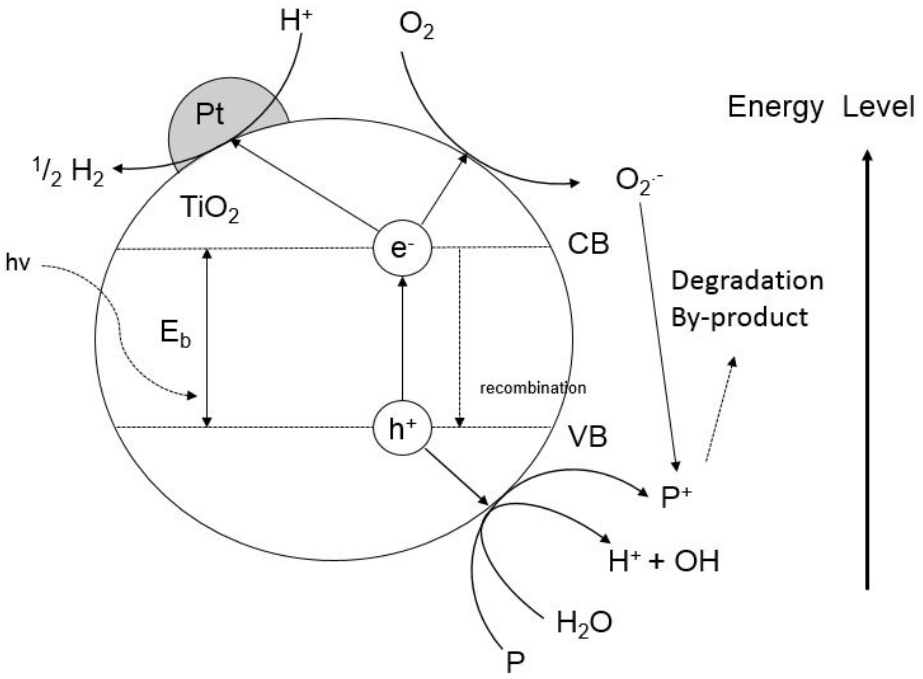

Figure 1.1: Schematic representation of the photocatalytic mechanism in the case of platinized titanium dioxide. Photons with the energy hv or higher reach TiO_2 and promote an electron from the VB to the CB. The created electron-hole pair can recombine and exhaust the excess energy in form of heat or a photon or move to the surface. With reactants adsorbed at the catalyst's surface the electrons and holes can perform a reaction by either reducing or oxidizing the reactants. The platinum loads act as electron scavengers and reduce the over potential for H_2 formation [9]

Photocatalysis is relative similar to normal catalysis only that the catalyst needs light for its catalytic function to work. The photocatalytic process can be classified into five independent steps:

- Transfer of the reactants in the fluid phase to the surface.
- Adsorption of at least one of the reactants.
- Reaction in the adsorbed phase
- Desorption of the product(s).
- Removal of the products from the interface region.

Usually, the third is the rate limiting step which allows to neglect steps 1, 2, 4 and 5 and purely focus on the photocatalytic reaction [2].

1.1.3 Characteristics of TiO_2 as a photocatalyst

From a range of materials TiO_2 is one of the most promising semiconductors for photocatalysis. With its high chemical stability, low cost, water insolubility, safety towards human and environment it possesses ideal properties for photocatalytic processes [10][11]. It commonly appears in three different types of crystal structures, anatase, rutile and brookite, having band gaps of 3.2, 3.02 and 2.96 eV, respectively. The anatase crystal structure is most active for photocatalysis, however, mixing the anatase and rutile phase in a 75% and 25% ratio is said to improve the catalytic activity. A mixture of anatase and rutile has defects in the crystal structure

which act as electron traps with an effect that increases the electron-hole life time [12]. Figure 1.2 shows that the band gap of TiO_2 is in a position which favors the production of many species such as hydrogen and oxygen making this semiconductor suitable for a broad range of applications.

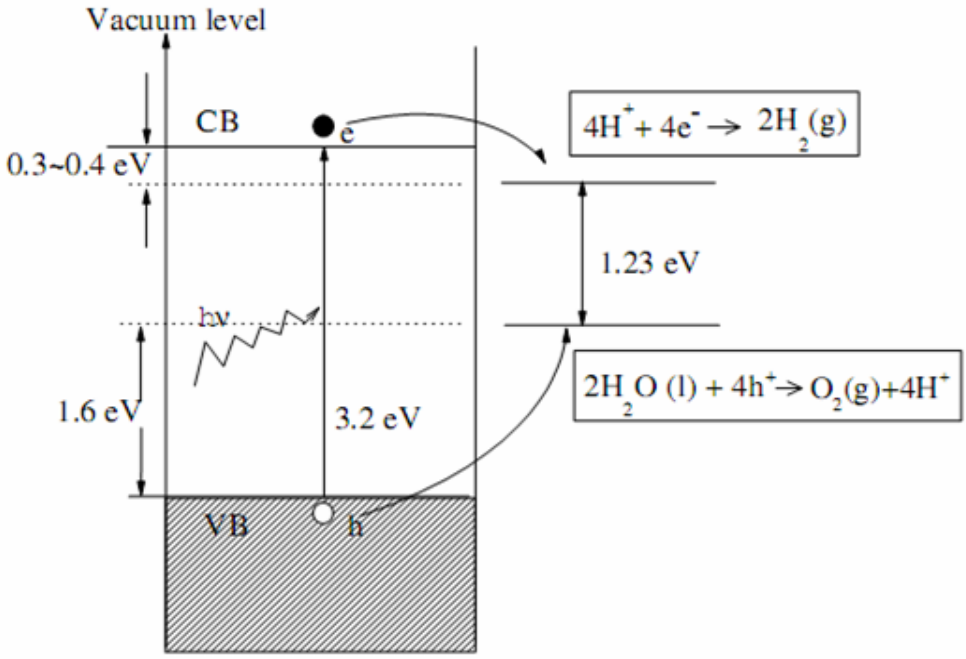

Figure 1.2: Band gap of anatase TiO_2. An excited electron has the potential to reduce protons to hydrogen and the hole can split water to form oxygen [13]

1.2 Aims and Approach

This bachelor research focuses on the degradation of organic contaminants in water combined with hydrogen production. This purpose is approached by loading platinum on TiO_2 via photodeposition and testing the sample by performing photocatalytic degradation reactions of organic compounds (formic acid, methyl orange and acid orange). The photocatalytic degradation of organic compounds were followed using UV-Vis spectrometry. In parallel, similar reactions were conducted in a reactor connected to a gas chromatograph (GC) connected with a thermal conductivity detector (TCD) to follow the hydrogen evolution. XRD is used to characterize crystal properties of the catalyst.

2 Theoretical background

This chapter presents an theoretical overview of the techniques and technologies used for the research purpose of the bachelor assignment.

2.1 Photodepositon

Photodeposition uses the same principle as photocatalysis which starts with the excitation of electrons in TiO_2. Platinum group metal salts with a positive charge accept the electron which resides in the conduction band resulting in metal deposition. Sacrificial electron donors as methanol or ethanol are used to fill the positive hole in the valence band. For the loading of TiO_2 chloroplatinic acid forms the precursor and methanol acts as an electron donor in the photodeposition process [14]. The process can be expressed in the following form [9]:

$$M^{n+} + \text{SED} \xrightarrow[\hbar\nu \geq E_{bg}]{\text{semiconductor}} M\downarrow + \text{products} \tag{2.1}$$

A scheme of the process can be seen in Figure 2.1

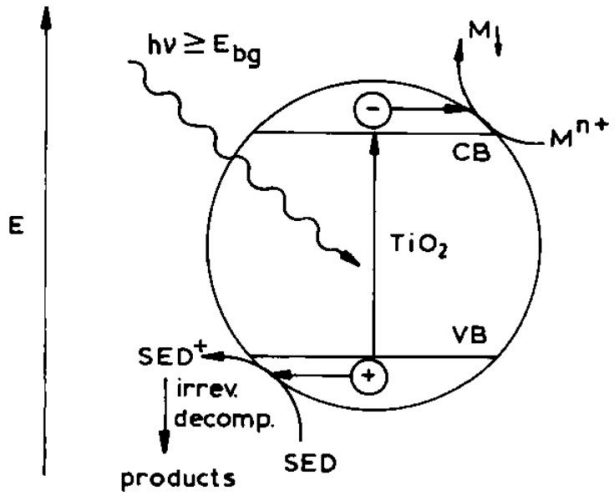

Figure 2.1: electron excitation by UV light allows metal deposition ($M^{n+} \rightarrow M\downarrow$) onto the semiconductor surface. Sacrificial electron donors (SED) are sensitized by the created hole [9].

2.2 UV-Vis spectroscopy

The UV-Vis spectroscopy can be used to identify the concentration of a compound in a solution. By illuminating the solution with monochromatic light with varying wavelengths the absorption is determined which can be related to the concentration by the beer-lambert law. This law is expressed as follows:

$$A = \epsilon b C \tag{2.2}$$

with:

A = absorbance
ϵ = molar extinction coefficient
b = path length
C = concentration

By creating a solution with known concentration of its content the molar absorption coefficient can be determined using the biggest absorption band of the spectrum. The determined coefficient can be used to determine the concentration of compounds during degradation allowing to create a concentration profile over time [15].

2.3 GC-TCD detector

Gas chromatograph with a thermal conductivity detector (GC-TCD) describes a technique for sample separation with subsequent quantity analysis. Gas chromatography allows the separation of compounds which can be vaporized without structural changes. Compounds to be analyzed are carried in an inert gas phase and show different interactions with a film at the wall. The separation happens by delayed arrival of the analyzed compounds which is a result of the interaction with the wall. Difference in solubility causes components in a gas stream to show different affinities for the stationary phase [16]. In combination with a TCD the separated compounds can be analyzed. By measuring the thermal conductivity of the medium and comparing it to a reference the concentration of a certain material can be deduced based on the difference in conductivity. This is done by heating the gases with a coil and determine the heat flow into the gas [17]. Usually helium is used as a carrier gas, however, when measuring hydrogen, argon is better suited due to the bigger difference in thermal conductivity [18].

2.4 XRD

XRD is a non-destructive analytical method to determine the phase composition and crystallinity of a material. The principle is based on braggs law which relates the wavelength of light to the incidence angle and the crystal layer thickness:

$$n\lambda = 2d \sin\theta \tag{2.3}$$

with:

n = order
λ = wavelength
d = layer thickness
θ = angle with respect to the plane's normal

When equation 2.3 is fulfilled diffraction takes place meaning that light is reflected constructively. This technique can be used to find out the microstructure and composition of materials and coatings by comparing the light intensity spectrum with data-bases which contain characteristic information about materials [19]. Heat treatment in the range of 600-700° leads to a phase transformation from anatase to rutile [20]. Since no high temperatures are involved in the photodeposition process no crystallinity changes are expected meaning that the XRD measurement should show similar results for the various batches of platinized TiO_2.

3 Experimental procedure

3.1 Platinum loading on TiO_2

Synthesis of platinized TiO_2 was done by photodeposition with subsequent centrifuging and drying. This section will describe the synthesis procedure which consists of platinum loading and solid-liquid separation.

3.1.1 Photodeposition

A photodeposition technique is used to load platinum particles onto TiO_2's surface. A batch is prepared which contains 1 g commercially available AEROXIDE® TiO_2 P25. Hexachloroplatinic acid ($H_2PtCl_6 \cdot (H_2O)_6$), the precursor, is added in dissolved form (concentration: 0.5 g L^{-1}) to the batch. The reactor is filled with MilliQ water to cover a volume of approximately 50 ml resulting in a TiO_2 concentration of 20 g L^{-1}. The amount of hexachloroplatinic acid taken was 20 ml, 52.6 ml and 0 ml to get a platinum loading of 0.4 wt %, 1 wt % and 0 wt %, respectively. Under constant stirring at around 350 rpm 30 minutes adsorption time was given. Next, methanol which functions as an electron donor was added and the system was illuminated with a 50 W HBO mercury lamp (Zeiss, 46 80 32 - 9902) given a photon flux of 2.77 10^{-8} Einstein $cm^{-2}s^{-1}$. The 0.4 wt % platinum loaded catalyst was independently synthesized three times to check for reproducibility. A scheme of the process is displayed in Figure 3.1

3.1.2 Separation by centrifuging and drying

To recover the sample the slurry, containing platinized TiO_2, was centrifuged for 30 min and the excess solution containing water and chlorine ions was separated from the deposit. The solution was centrifuged again to save traces of the catalyst. The slurry was washed with ethanol separated by centrifuging, washed with MilliQ water and centrifuged in an alternate fashion in total 3 times. To evaporate traces of solvents in the sample it was dried in an oven at 80°C for 4 hours .

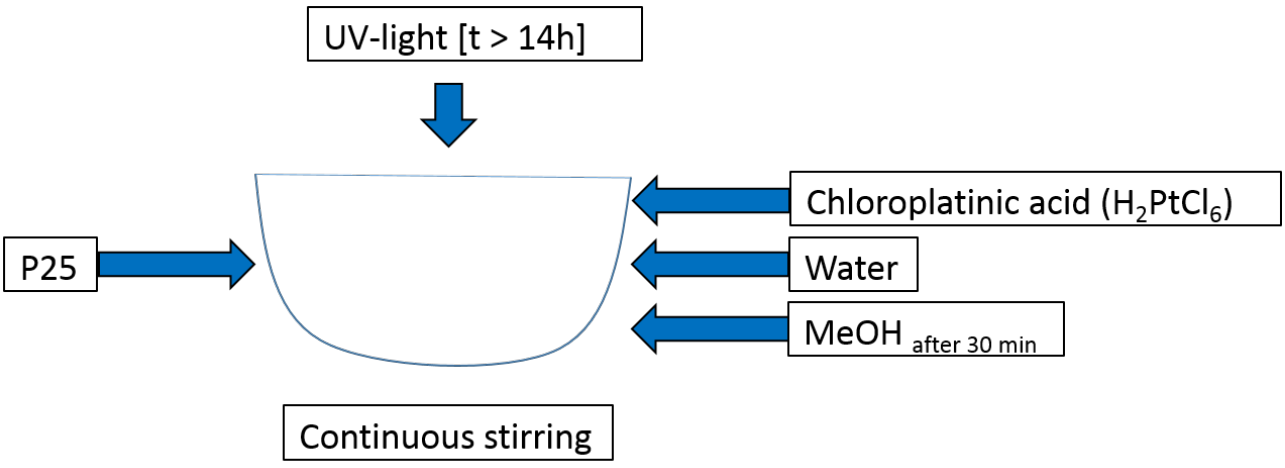

Figure 3.1: Sketch of the setup for photodeposition

3.2 Photodegradation

In order to evaluate the activity of the synthesized catalyst, degradation reactions are performed. Stirring time in the dark for 30 min is given to achieve adsorption/desorption equilibrium after adding the catalyst to solutions containing formic acid, methyl orange and acid orange 7, respectively. The solute concentrations are specified in Table 3.1 with a reactor volume of 50 ml. Each solution is tested with the three synthesized catalysts. One extra degradation test was done with untreated P25 and a methyl orange solution. UV illumination is performed for about 90 to 120 minutes with a light intensity at the liquid surface of 3.21 mW cm^{-2} and a wavelength range of 360 to 380 nm. During the adsorption and illumination the system is continuously bubbled with oxygen at a rate of 50 ml min^{-1} and magnetically stirred at a rate of 350 rpm. The absorption spectra of the samples were determined for pure solutions, after reaching the adsorption/desorption equilibrium and after 5, 10, 15, 30, 60, 90 and 120 minutes of UV illumination. The sample extraction was performed using a syringe and a tube connected to the solution. Prior to the UV-Vis spectrometry analysis with UV cuvettes all samples have been filtered to remove the catalyst. Residues in the tube were flushed back into the reactor. Prior to absorption measurements of the pure solution it was filtered for consistency reason, too. Some of the degradation experiments were repeated for reproducibility tests. A schematic configuration of the experimental setup is shown in Figure 3.2. Table 3.1 gives a summary of the exact experimental conditions.

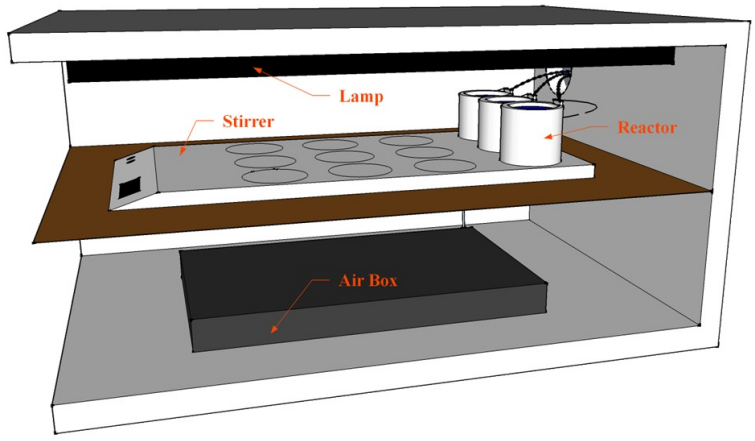

Figure 3.2: Schematic presentation of the degradation reactor with UV lamps, air flow, stirring plates and an tube for sample extraction

Material	Concentration	Reactor volume in ml	Air flow in ml min^{-1}
n wt %Pt-P25	0.25 $^{g}/_{L}$	50	50
Methyl orange (MO)	$3.05{\cdot}10^{-2}$ mM		
Acid Orange 7 (AO)	$3.05{\cdot}10^{-2}$ mM		
Formic Acid (FA)	5.31 mM		

Table 3.1: Summary of the degradation reaction specification

3.3 GC with TCD for hydrogen quantification

Similar degradation tests were performed in a system consisting of a reactor (volume size: 15 ml) connected to a compact gas chromatograph equipped with a thermal conductivity detector (GC-TCD) and a valve system

controlled by a LabView user interface [21]. Figure 3.3 shows an arrangement of 4 photoreactors and the Gas chromatograph (white box to the right) with channels for gas transport connecting the reactor and the GC. The black cords are optical fibers which transport the light from the source. The TCD was calibrated for hydrogen detection. Batches with pure water, methyl orange (10 mg L^{-1}) and once with acid orange 7 (10.5 mg L^{-1}) in combination with 1 g L^{-1} platinized TiO_2 were illuminated with UV-light (120 W mercury lamp) while using argon as a carrier gas at a flow rate of 42 ml min^{-1} and a stirring rate of 250 rpm. Some reactions were conducted with methanol or formic acid as a sacrificial agent. The reaction was set to run for 72 minutes with sample analysis every 80 sec to measure the amount of hydrogen in the gas phase. Before and after illumination the pH of the slurry was determined. The exact experimental configuration is displayed in Table 3.2. Due to the consumption of the 0.4 wt %Pt-P25 catalyst and problems with reproducibility it was necessary to conduct some of the tests with the 1 wt % Pt-P25 catalyst.

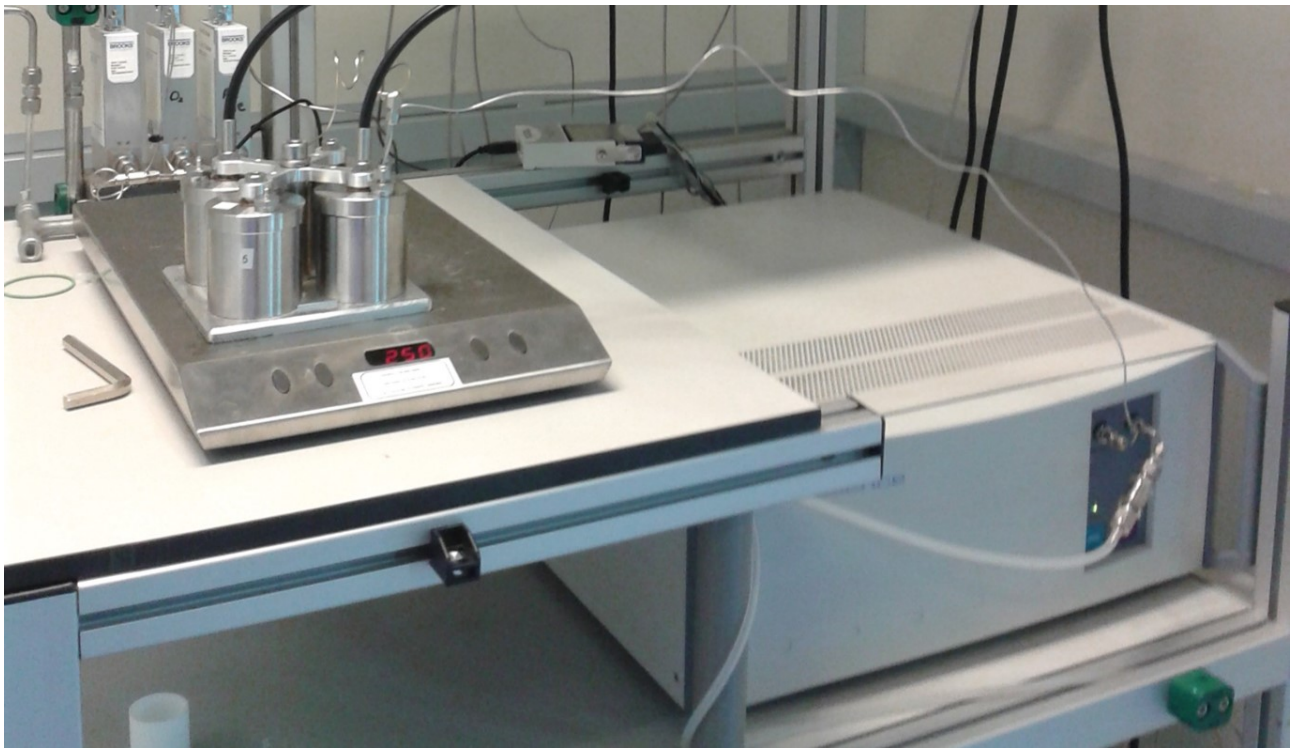

Figure 3.3: Setup used for photodegradation and hydrogen production

No.	Solution	sacrificial agent	Catalyst	Extras
1.	H_2O (15ml)	—	0.4 wt %Pt-P25	
2.	H_2O (14.5ml)	MeOH (0.5ml)	0.4 wt %Pt-P25	
3.	H_2O (14.5ml)	FA (0.466ml)	0.4 wt %Pt-P25	
4.	H_2O (14.5ml)	FA (0.466ml)	1 wt %Pt-P25	
5.	MO (15ml)	—	0.4 wt %Pt-P25	
6.	MO (14.5ml)	MeOH (0.5ml)	P25	
7.	MO (14.5ml)	MeOH (0.5ml)	0.4 wt %Pt-P25	
8.	MO (14.5ml)	MeOH (0.5ml)	1 wt %Pt-P25	
9.	MO (14.5ml)	MeOH (0.5ml)	1 wt %Pt-P25	adjusted pH by adding HCL
10.	MO (14.5ml)	MeOH (0.5ml)	1 wt %Pt-P25	injection of 0.75ml $200^{mg}/_{L}$ MO after 30 min
11.	MO (14.5ml)	FA (0.466ml)	0.4 wt %Pt-P25	
12.	MO (14.5ml)	FA (0.466ml)	0.4 wt %Pt-P25	no UV illumination
13.	MO (14.5ml)	FA (0.466ml)	0.4 wt %Pt-P25	additional 8 $^{ml}/_{min}$ oxygen bubbling
14.	AO (14.5ml)	MeOH(0.5ml)	1 wt %Pt-P25	

Table 3.2: Summary of the degradation reaction setup

3.4 Catalyst characterization by XRD

XRD measurements are performed on the different samples to see if Pt peaks can be recognized and to see if the crystalline phase changes with different platinum loadings. XRD patterns were recorded using a Bruker D2 PHASER spectrometer. The measurements were done from 10° to 90° using a step size of 0.25°.

4 Results

4.1 Platinum load on TiO_2

In total five batches of catalyst were prepared one without any platinum loading, one with 1 wt %Pt load and three with 0.4 wt %Pt load. The obtained catalysts show an increase in grey scale compared to the commercial P25 TiO_2. Grey level increase is noticeable for increasing platinum loadings and grey level fluctuations are present for the three batches of 0.4 wt %Pt - P25. Figure 4.1 shows the obtained samples after photodeposition. After separating the solution from the catalyst after centrifuging a dark grey layer was observed at the catalyst's surface. The resulting solid sample after drying showed also a darker grey layer than the color inside. The material loss associated to photodeposition is 11.8% for a platinum weight load of 0.4%, 12.1% for 1% platinum load and 5.8% for no platinum load. The reproduced 0.4 wt %Pt-P25 batches show big variations in grey color which is unexpected since all photodeposition conditions were the same.

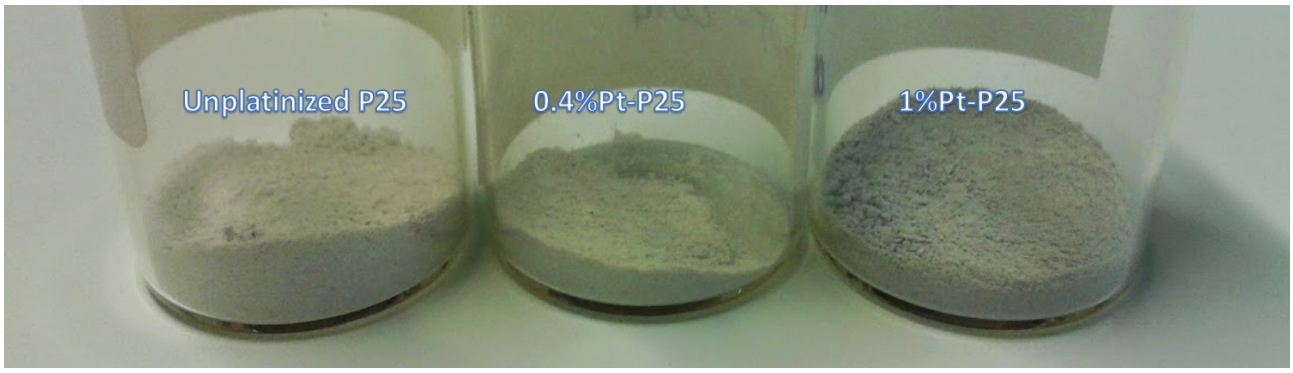

Figure 4.1: TiO_2 powder with different platinum loadings

4.2 Catalyst crystallography

XRD analysis allows to see if structural changes appear due to treatment procedures and platinum loading. Anatase and rutile structures have their own characteristic angles at which peaks appear. Strong diffraction peaks for rutile are expected at 27°, 36° and 55° whereas, anatase should show strong peaks at 25° and 48° [22]. The XRD spectrum of the three catalysts with different loadings can be seen in Figures 4.2a, 4.2b and 4.2c. Included in the figures is a characterization of the peaks which represent either the anatase or rutile crystal and the corresponding crystal plane. As expected, clear peaks for rutile and anatase can be seen at the mentioned angles. Furthermore, less distinct peaks are assigned to one of the crystal structures by comparing the XRD spectra of pure rutile and anatase with the obtained XRD results [22]. The spectra, compared to each other, hardly show any variation such that it can be concluded that the platinum load up to 1 wt % does not have any influence on the crystallinity of the catalyst. A difference between the plots can be seen in the strength of the peaks. The peak at 25 ° reaches a value of 11000 for pure TiO_2, 14500 for 0.4 wt % platinum load and 12500 for 1 wt % platinum load. E. Pulido Melián claims to detect characteristic Pt peaks at angles of 40.0, 46.5 and

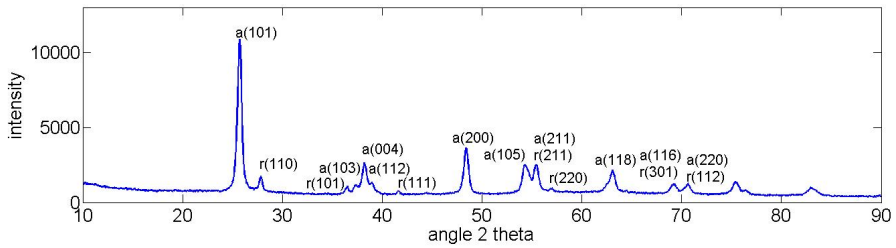

(a) XRD spectrum for unplatinized TiO_2 P25

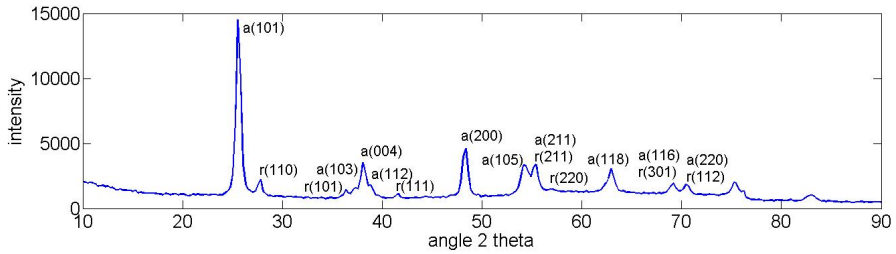

(b) XRD spectrum for 0.4%Pt-P25

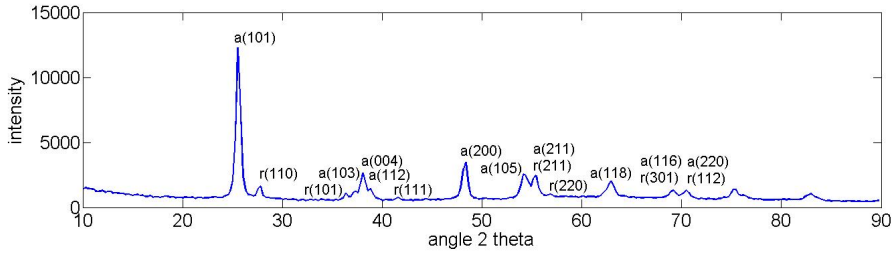

(c) XRD spectrum 1%Pt-P25

Figure 4.2: XRD spectrum for unplatinized, 0.4% and 1% platinum loaded TiO_2

67.9 [23]. The XRD spectra in Figure 4.2a, 4.2b and 4.2c do not show this characteristic behavior which means that no conclusion about the platinum load based on that method can be drawn.

4.3 Degradation results

The spectrometry results show that the maximum light absorption occurs at wavelengths of 463 nm, 485 nm and 216 nm for methyl orange (MO), acid orange (AO) and formic acid (FA), respectively. The absorption spectrum for FA showed some fluctuations compared to MO and AO. Time t = -30 refers to the point where the catalyst was added to the solution and t = 0 refers to the point where the light illumination starts. The change in solute concentration based on the decrease in the absorption spectrum for the three compounds can be seen in Figure 4.3a for methyl orange, Figure 4.3b for acid orange and Figure 4.3c for formic acid. A stirring rate of 350 is sufficient to provide maximum solute-catalyst interaction [24].

MO in contrast to the other compounds, shows hardly any absorption decrease between time t = -30 and t = 0. The degradation speed of MO and AO is fast enough to degrade nearly everything of the compounds within 90 minutes, whereas, formic acid can be detected even after 120 minutes which was expected since the initial concentration was much higher.

Using the beer-lambert law it was possible to calculate the solute concentration. The molar extinction coefficient was determined by taking the concentration of the diluted organic compounds (MO, AO and FA) together with the maximum absorption value. Since the same cuvette was used for all measurements the path length was constant and could be divided out of equation 2.2. The calculated values for ϵ were found to be 23410 L mol^{-1} cm^{-2} for MO, 18492 L mol^{-1} cm^{-2} for AO and 33 L mol^{-1} cm^{-2} for FA. The molar extinction coefficient together with the absorption at the wavelengths where the maximum for t = - 30 was measured allows to determine the concentrations after adsorption and different illumination durations. Plotting

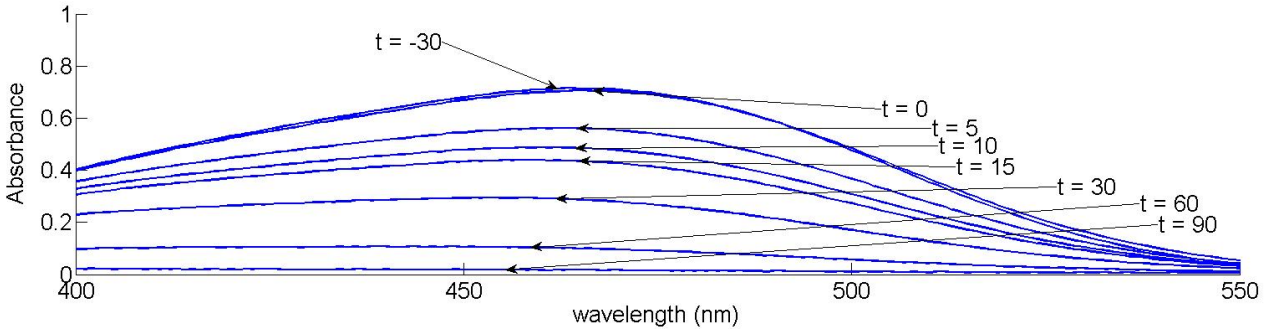

(a) MO absorption spectrum for various degradation times with 0.4%Pt-P25

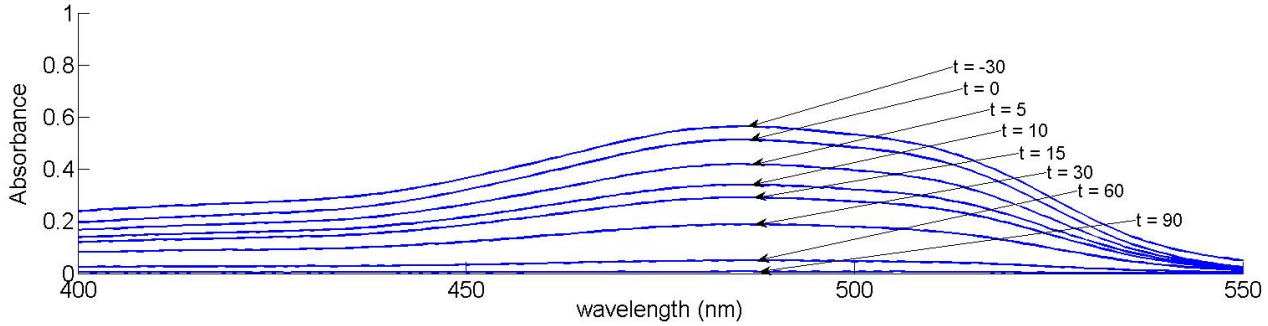

(b) AO absorption spectrum for various degradation times with 0.4%Pt-P25

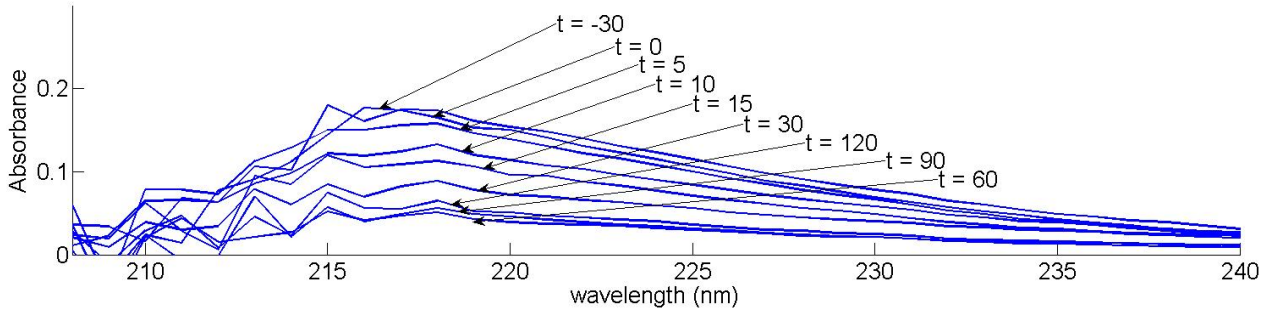

(c) FA absorption spectrum for various degradation times with 1%Pt-P25

Figure 4.3: Absorption spectrum for MO, AO and FA

all concentrations for MO, AO and FA in combination with 0 wt %, 0.4 wt % and 1 wt % platinized TiO_2 results in the degradation profiles shown in Figure 4.4:

The experimental results show that solute degradation rates increase when loading the semiconductor with platinum. A comparison between TiO_2 without treatment and with experienced photodeposition shows that the process decreases photoactivity. Therefore, the treated catalyst was used as a reference instead of normal TiO_2 P25. Degradation tests on MO and AO show an increasing adsorption trend on the catalyst for increasing amounts of platinum deposited. The degradation rate of MO increases when using a platinized catalyst but no big performance difference was observed between the 0.4% Pt and the 1% Pt load. AO shows fastest degradation kinetics when using a 1% Pt catalyst and the 0.4% Pt catalyst has a slightly lower degradation performance. The concentration profile for the two organic substances shows a logarithmic decrease.

Unlike MO and AO did FA show unique behavior. Five minutes after turning on the lamp the concentration went up before it started to degrade. This trend could be observed for various degradation tests with FA. It can be seen that the catalyst with 1% platinum load shows a distinct improvement for formic acid degradation whereas, the 0.4% platinum load shows nearly no improvement.

To investigate the reproducibility of the photodeposition method degradation tests with the three 0.4 wt % Pt-P25 batches were conducted using MO as a reactant. The degradation results are shown in Figure 4.5. There is a distinct variation in degradation rate although having in theory the same platinum loading on the

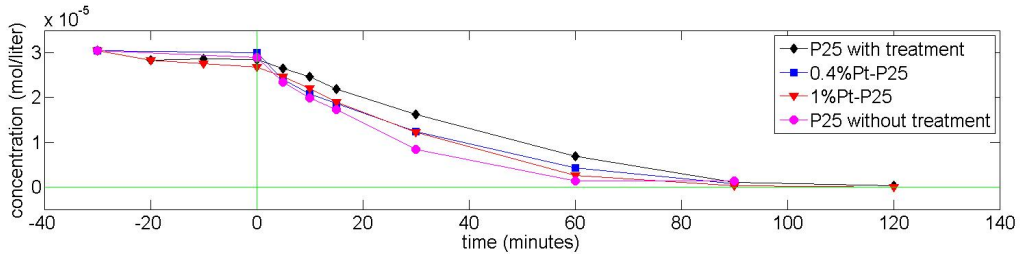

(a) MO degradation using TiO_2 with different platinum loads

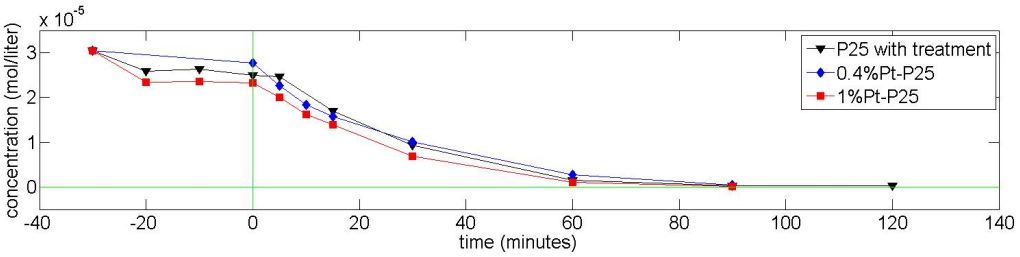

(b) AO 7 degradation using TiO_2 with different platinum loads

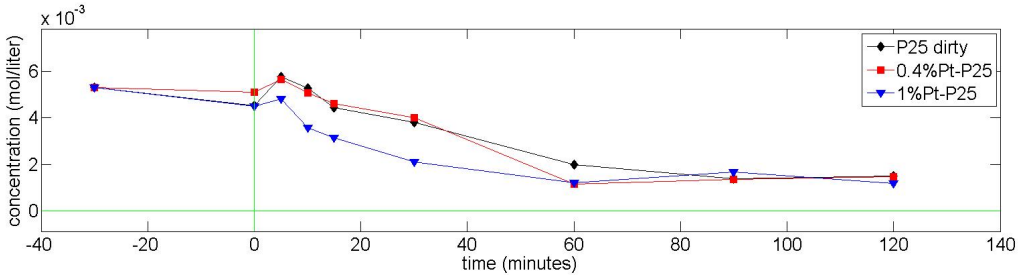

(c) FA degradation using TiO_2 with different platinum loads

Figure 4.4: Overview for degradation for TiO_2 with various platinum loads

catalysts. It is noticeable that the catalysts from this test with the lowest photoactivity had also the darkest grey level.

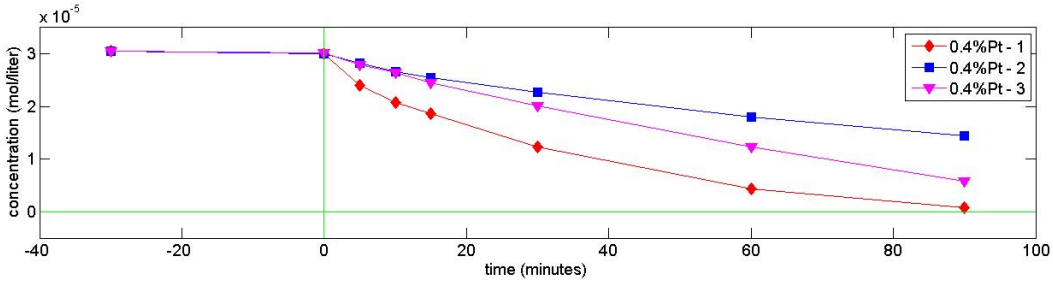

Figure 4.5: Degradation test with three different 0.4 wt %Pt-P25 catalysts and MO

4.4 Hydrogen production

With the aid of a calibration curve detected hydrogen signals were transformed into concentration values in ppm. The results show that the platinum loading and the addition of an electron donor favors the production of hydrogen. When non platinized TiO_2 was used regardless if sacrificial agents were present a negligible amount of hydrogen was detected. The same observation was done when methanol or formic acid as a sacrificial agent was absent. After an illumination time of 72 minutes all tests with MO resulted in complete decolorization. In general, it could be noticed that when the UV light was turned on the hydrogen production showed an overshoot before it settled to a fix value. As can be seen in Figure 4.6 there is a higher overshoot and a higher steady-state hydrogen production (40 ppm and 22 ppm) for MO compared to water with only 20 ppm and 13

ppm, respectively when methanol as a sacrificial agent is added to both solutions. Performing the same test with adding the same molar amount of highly concentrated MO after 30 minutes reveals that another hydrogen concentration peak appears in the argon stream, but settles again at the same level as before injection. Tests using 0.4 wt % Pt-P25 and 1 wt % Pt-P25 show that hydrogen production rates are at the same level.

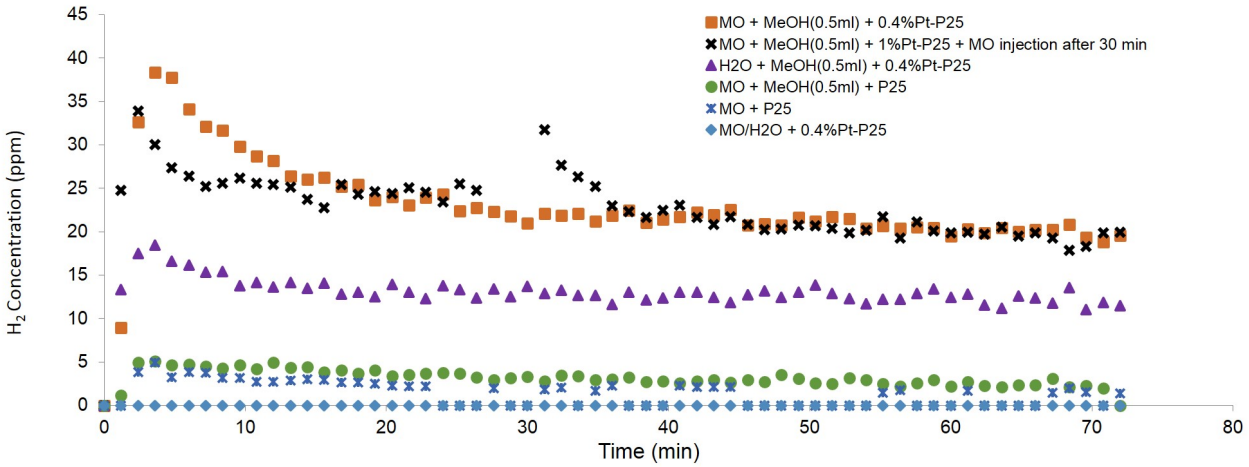

Figure 4.6: hydrogen concentration in argon as a result of the photocatalytic degradation of pure water, MO and mixtures of the substances with methanol.

Solutions with methanol exhibited a pH of 5 and solutions with FA a pH of 2. A comparison of sacrificial agents reveals that FA shows with 22 ppm a higher hydrogen production than methanol in water with 13 ppm. When MO as a pollutant is present the hydrogen production with FA drops to a level of 13 ppm and rises with methanol to a level of 22 ppm. Hydrogen chloride was added to the MO-methanol mixture such that the pH was at a level of 2 which resulted in a hydrogen production lower than that for a mixture of MO and FA. Measurements of the pH before and after the photocatalytic degradation show that the pH value of the system did not change. The obtained results are represented in Figure 4.7

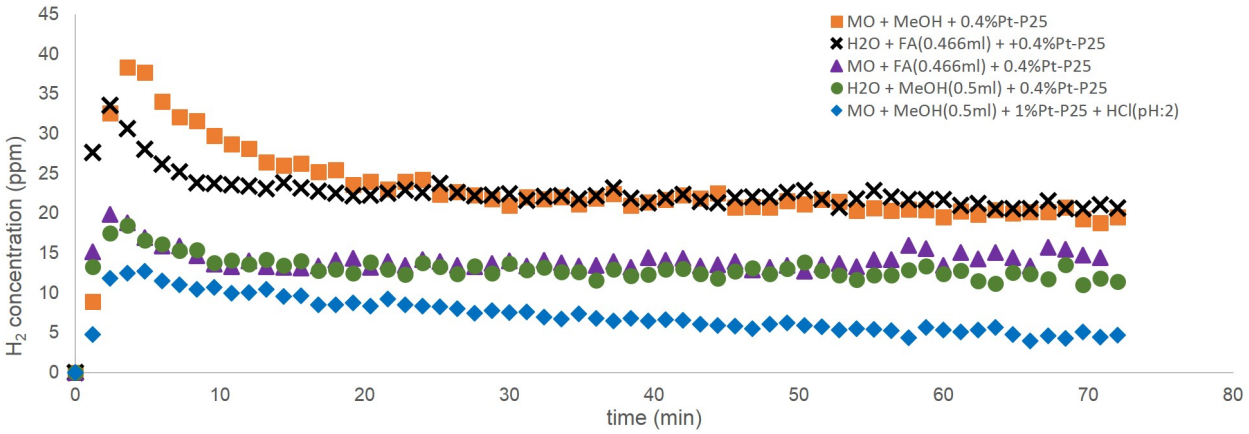

Figure 4.7: Comparison of hydrogen concentration in argon as a result of the photocatalytic degradation of water and MO with methanol and FA as a sacrificial agent.

The combination of MO and FA changes the solution color from orange to red and results in decolorization when adding the catalyst while no illumination takes place in less than 30 minutes. When adding oxygen to the argon stream the red color stayed. No hydrogen could be detected when light illumination was left out, showing that the decolorization is not related to the production of hydrogen. When oxygen was added the hydrogen concentration showed no overshoot but settled to a stable level of about 5 ppm. With argon as the only component of the gas stream, the hydrogen concentration went first up to 20 ppm before it settled at about 14 ppm. The results are shown in Figure 4.8.

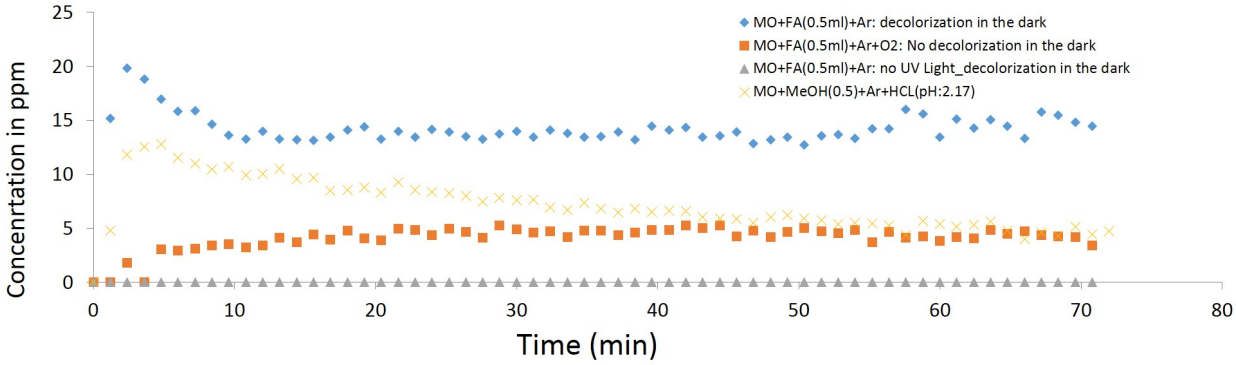

Figure 4.8: hydrogen concentration in argon as a result of the photocatalytic degradation of MO with formic acid

To understand the effect of methanol and FA on the degradation rate the same tests as in the hydrogen tests were conducted with the focus on degradation speeds. Figure 4.9 shows that the degradation rate of a mixture of MO and FA is much faster compared to MO with methanol or MO alone. Successful degradation was achieved within 3 minutes, however, FA was still present in such high concentration that degradation rates for this compound could not be determined over a time span of 45 minutes. The addition of methanol showed no changing effect on the degradation speed of MO with complete decolorization in the range of 25 minutes using a catalyst load of 1 g L^{-1}.

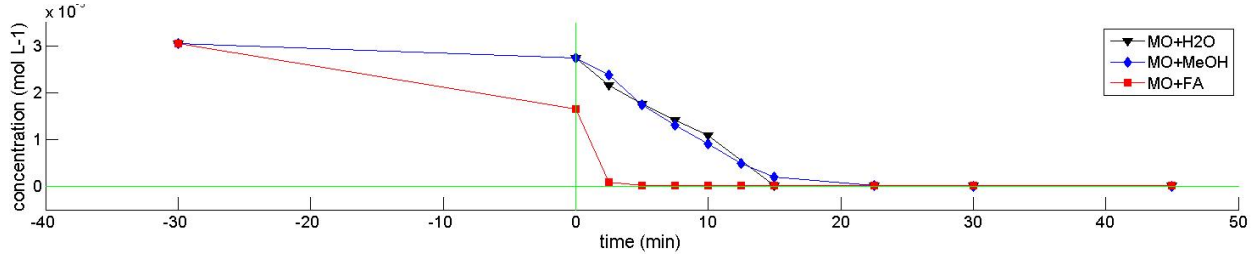

Figure 4.9: Degradation test of MO alone, with methanol and formic acid

To see if the behavior of MO on hydrogen production can be extended for dyes in general another test with AO was conducted. It shows that hydrogen production increases compared to a system with water and methanol only, but it cannot reach the same performance as MO. The result is represented in Figure 4.10:

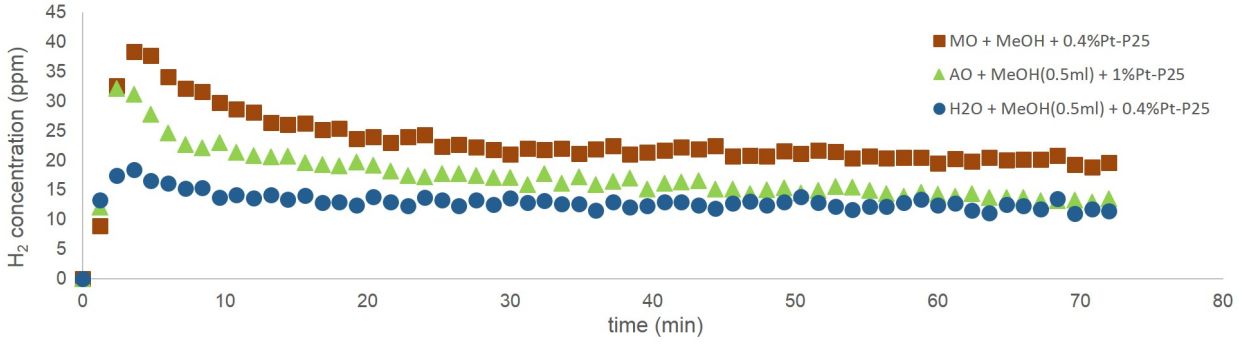

Figure 4.10: Hydrogen production for MO, AO and water in combination with methanol

5 Discussion

5.1 Catalyst synthesis

The apparent grey color which could be observed for platinized TiO_2 is in agreement with literature and indicates the deposition of platinum on the catalyst [25]. From the varying photocatalytic tests using independently synthesized 0.4 wt % Pt on TiO_2 it can be seen that the reproducibility of platinum loading by photodeposition is poor. One reason for this result can be the photodeposition reactor. A stable stirring and position of the light source on top of the reactor were two parameters which were difficult to keep always the same. The dark grey layer present directly after centrifuging and after drying shows that the platinum load was not deposited uniformly. Alternatively, other loading processes could have been used such as impregnation [9]. The crystallinity stayed unaffected when loading platinum on the catalyst. The load was not high enough to detect it using XRD unlike stated by E. Pulido Melián but is consistent with other observation which claim that a minimum load of 5 wt % is required. However, the increase in peak height with platinum load is consistent with other observations in literature which proves next to the grey color platinum presence [26].

5.2 Photocatalytic activity

The experimentally determined values for the wavelength with the maximum absorption for MO at 463 nm and AO at 485 nm agree with literature values [27][28]. As shown in the results does FA show noise in the range of 200 to 215 nm. In literature is reported that the maximum absorption band is at 210 nm, due to instability of the signal at that wavelength the value at 216 nm was used [29].

Parameters which influence the rate of degradation are the stirring rate, amount of catalyst, amount of platinum loaded, type and amount of reactant degraded [24][30]. Degradation kinetics for MO, AO and FA show that the platinum load has an enhancing effect, however the effect of platinum loading shows only a minor improvement which stands in contrast to many claims in literature [9]. One reason for that result might be the structural composition of the type of TiO_2 employed. TiO_2-P25 is already optimized with the mix of rutile and anatase for electron-hole separation. The good electron-hole life time results from a band shift between rutile and anatase. The CB of the rutile crystal structure has a higher negative potential such that electrons reduce their energy when moving to the anatase crystal. The positive potential of the VB is lower for rutile such that holes are trapped in this crystal [12]. It is even said that platinum could have a negative effect by reducing the active sites of TiO_2 [30]. Other TiO_2 compositions as Hombikat, a 100% anatase crystal with high specific surface area, show in general better improvement with platinum loadings [30].

Since MO shows nearly no improvement when increasing the platinum from 0.4 to 1 wt % it can be concluded that higher loadings will not show any improvement. Comparative studies found an optimum platinum load of 0.75 wt % for most efficient degradation [7]. AO and FA show a bigger improvement for the 1 wt % Pt-P25 and it might be that higher loadings could enhance the degradation rate of those compounds even more. At low concentrations platinum traps successfully electrons, however at higher loadings recombination starts to increase because the average distance of trap sites decreases and agglomeration effects appear [7]. Another effect which appears at high loadings is blocking of light such that less electrons can become excited [31]. This

unique behavior tells that each reactant to be degraded has a different optimal platinum concentration making each system individual such that conclusions about the optimal platinum loading cannot be drawn on a general level. Next to the type of reactant used the type of TiO_2 employed can show different photoactivity changes when loaded with platinum. This unique characteristics led already to much controversion and conflicting observations [30].

Oxygen employed in the photocatalytic reaction gets reduced by the electron in the CB while organic compounds as MO, AO and FA go through an oxidizing reaction which happens at the hole in the VB [3]. Degradation without oxygen will result in accumulation of negative charges which results in an increase of electron-hole recombinations and leads to a decrease of the quantum efficiency of the catalyst lowering the degradation rate [3].

The low adsorption of MO onto the catalyst indicates that the degradation reaction is dominated by indirect oxidation. In an alkaline solution MO is negatively charged. With the presence of TiO^- groups on the catalyst surface MO is weakly adsorbed due to Coulombic repulsion [32]. When illuminated with UV light, TiO_2 is capable of generating hydroxyl radicals, a strong oxidant, which possesses the function to react with organic reactants when desorbed from the catalyst's surface [33]. AO and FA show higher adsorption behavior, however it is difficult to make clear interpretations about the observations of the three compounds because three types of reaction mechanisms can occur: (1) attack by a hydroxyl radical, (2) direct oxidation by the positive hole or (3) direct reduction by the electron in the conduction band [32].

An interesting observation was the rise of FA before the concentration went down after turning on the light. There are two possible explanations for this phenomenon. The first is that turning on the light starts to desorb FA from the catalysts surface and the second is that the spectrometry measurement was detecting two compounds at the same time with absorption spectra in the same range. It might be possible that concentration rise is attributed to the formation of hydrogenperoxide (H_2O_2) which has an absorption spectrum in the same range as FA [34]. The formation of hydrogenperoxide cannot be excluded since the degradation tests where always conducted in an oxygen rich system which by reduction can result in H_2O_2 formation [3]. A possible reaction mechanism for the formation of H_2O_2 might be the reaction of superoxide with two protons in two steps [8]. Electron microscopy could have been employed to get images which allow conclusions about the range of particle sizes of the catalyst.

5.3 Coupling hydrogen production with dye degradation

The tests on hydrogen production show that platinum plays a crucial role in that process. Although, the load showed only small effects on photocatalytic activity for dye degradation it is necessary for hydrogen production. The goal is to combine the degradation of organic compounds and hydrogen production. One application for hydrogen produced is to use it in a catalytic reaction for nitrated and nitrites degradation [35].

Tests with non platinized TiO_2 show no hydrogen evolution which is evidence for the catalytic functionality of platinum in the reduction process of protons to hydrogen [8]. However, only in the presence of sacrificial agents it was possible to produce noticeable amounts of hydrogen which results from an effective electron-hole separation by the donation of electrons [36].

The initial peak in hydrogen evolution was also observed by other groups. Decrease from the initial production rate might be associated with deactivation of the catalyst. A test by Galinska et. al [36] showed that the hydrogen production stopped after a certain amount of time and continued when a new batch of platinized catalyst was added. The deactivation of the catalyst could be related to an accumulation of photogenerated species which cover the surface and hinder the production of hydrogen. The oxidation of water might form oxygen which gets reduced to superoxide ion and sticks to the surface of platinum, thus mitigates the production of hydrogen. Another possibility could be that the oxygen and hydrogen concentration starts to increase after turning on the light and thus, allows the formation of water [8]. When inserting more MO after 30 minutes another peak could be detected which proves that deactivation of the catalyst did not happen.

The high potential to split water (2 eV) is the reason why a lot of electron-hole recombination is present which results in the formation of water. Methanol has a lower splitting energy required (0.7 eV) and thus, shows better activity as an oxidized species and like water it an provide protons for hydrogen evolution [37]. The decomposition of methanol forms formaldehyde. In the presence of oxygen formaldehyde can form FA [25]. The pH measurements show that no changes occurred which agrees with the theory. The absence of oxygen did not allow to form FA which would have lowered the pH. The addition of MO enhances the hydrogen production rate. The possible reaction mechanics might look as follows: Photogenerated oxygen leads to the oxidation of the dye and is consumed until complete mineralization was achieved [8]. In the absence of a dye the hydrogen production is higher when FA is employed in comparison to methanol. This shows that the oxidation process from FA to hydrogen and carbon dioxide is faster than the formation of formaldehyde from water and followed by oxidation forming hydrogen and carbon dioxide [6]. The addition of MO to FA shows a mitigation of the hydrogen production but results in very fast decolorization. The decolorization can be explained with the higher adsorption affinity of MO to the catalyst surface in acidic environments due to the absence of coulombic repulsion forces as explained in the previous section.

When comparing the other two tests in Figure 4.9 with the degradation speed in Figure 4.4 it can be seem that the a higher catalyst concentration (1 g L^{-1} vs. 0.25 g L^{-1}) leads to a faster degradation rate. In literature it is reported that an optimum is achieved at a concentration of 2 to 2.5 g L^{-1} before screening effects can occur because the high solid density blocks the UV illumination which decreases the photoefficiency [2].

The lower hydrogen production trend under acidic conditions was also confirmed by tests with MO and methanol in the presence of hydrogen chloride. The mitigating effect of hydrogen production at low pH employing MO stands in contrast to Patsoura et. al who state that the amount of hydrogen production is proportional to the amount of dye added and that the trend is not affect by changing pH [8]. Although, the use of FA establishes the solution pH at 2 it shows better hydrogen formation ability than methanol at pH 5 which shows that a pH difference of 3 cannot hinder the better oxidation capability of FA over methanol.

The tests in which oxygen was added to the gas flow showed a low hydrogen production compared to tests with absent oxygen. This behavior can be expected since the formation of hydrogen and superoxide happens through reduction by an electron in the conduction band [10]. The introduction of oxygen enables the latter reaction and leads to a competition between these reactions as displayed in Figure 1.1 [38]. Although when not bubbled with oxygen decolorization occurs but no hydrogen could be measured when not illuminating the system with light which is logic when considering that decolorization comes from better adsorption behaviors. Next to the strong adsorption behavior also very fast degradation behavior can be observed. A possible explanation could be related in the split of the nitrogen double bond which is a characteristic property for azo dyes. That split can occur in the presence of a catalyst and another atom which can share the apparent free electron pair. Protons are well suited for this mechanism. The presence of acidic conditions provides a high concentration of protons promoting the splitting of the nitrogen double bond [39]. The reaction mechanism is displayed in Figure 5.1. That would agree with the fast degradation observation.

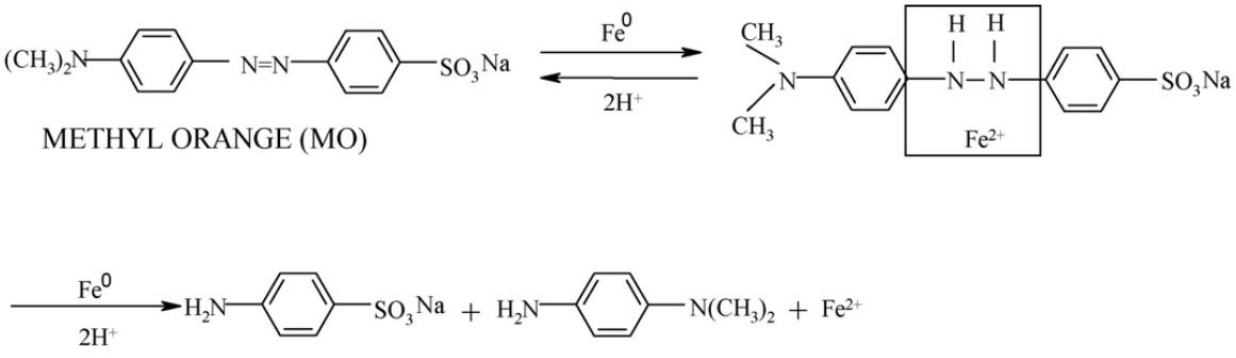

Figure 5.1: Reaction mechanism for the decolorization MO with Iron as a catalyst

The hydrogen production test with AO allows to make conclusions of dye degradation with coupled hydrogen production on a broader scale. The fact that the addition of AO increases the hydrogen production rate allows to make a more general statement about enhanced hydrogen production in the presence of dyes. The same trend was already confirmed by Patsoura et. al. [8]. However, it can be seen that MO produces more hydrogen than AO which shows that a separation between dyes has to be done when quantifying the hydrogen production rate.

The coupling of organic reactant degradation and hydrogen production was demonstrated successfully in this study, however, a trade off has to be made based on the pH of the solution. By adjusting the pH reciprocal effects for degradation rates and hydrogen production rates could be observed.

6 Conclusion

The research presented in this bachelor thesis shows that platinum has an enhancing effect on photo degradation activities. The actual effect depends on the reactant used for degradation. In general photocatalytic improvement showed a minor effect which is assumed to depend on the already good electron-hole life time of TiO_2-P25. The photodeposition method for platinum loading needs to be optimized. Evidence was shown for the catalytic functionality of platinum for hydrogen production. Next to platinum it is necessary to employ sacrificial agents as methanol or formic acid which allow the effective removal of holes to prevent water formation and the provision of protons due to low conversion potentials. The combination of organic pollutant degradation and hydrogen production showed that the process is affected by adjusting the pH of the solution. Low pH results in fast degradation kinetics but weak hydrogen production for MO. The type of oxidized species employed in photocatalytic reactions shows that the pH influence is dependent on the type of oxidized species employed. When only water is used the hydrogen production was higher with the use of FA at a pH of 2 compared to methanol resulting in a pH of 5. From the results obtained throughout the research it becomes evident that predictions on photocatalytic degradation rates and hydrogen production cannot be made unless all parameters: amount of catalyst, platinum load, type and concentration of pollutant, type and amount of sacrificial agent and pH are know. Experiments showed the successful degradation of organic compounds coupled with enhanced hydrogen production rates, however, a trade-off has to be made based on the pH of the solution resulting in either fast degradation or high hydrogen production rates.

7 Recommendation

7.1 Photocatalytic degradation

A major concern of the presented study was the reproducibility of the photodeposition process. Reactor improvements need to be done in order to improve the reproducibility of the samples prepared. Various reactor shapes could be tested to allow better stirring and a more effective light access. Effects of platinum load and photodeposition on surface area of the catalyst could be investigated by using the BET method. The comparison between untreated and treated catalysts with photodeposition shows a negative effect on the photocatalytic activity of the catalyst. That effect could be related to a change in surface area. In order to get a better understanding of the photocatalytic activity of platinized photocatalysts, especially with regard to potential future applications, more tests with different platinum loadings could be employed to get a clearer picture of the optimal platinum load for various organic compounds and hydrogen production rates. The effect of pH variations could be investigated by performing tests in acidic, neutral and alkaline conditions and derive reaction kinetics for various degradation parameters (platinum load, catalyst concentration, reactant concentration, kind of reactant, solution pH, etc.). In principle, is it possible to use the photocatalyst multiple times. Recovery and repeated tests or long duration runs could give rise about the lifetime of the catalyst. The unusual behavior of initial concentration increase when degrading FA could be further investigated. Test without oxygen bubbling might hinder the H_2O_2 production. An increase of degradation rate in the absence of oxygen would be a strong indicator for the production of H_2O_2 which was characterized as FA.

7.2 Hydrogen production

For a broader understanding of photocatalytic degradation and hydrogen production more materials could be used as pollutants and sacrificial agents. A trend could be recognized that higher pH values allow higher hydrogen production rates. Tests should be extended to more organic compounds under various pH conditions to study the hydrogen evolution. When employing acids as sacrificial agents such as FA, buffer solutions could be used to create alkaline conditions. One parameter which was not varied throughout the tests was the temperature. Higher temperatures are supposed to enhance the hydrogen production rate [8]. This effect could be tested by heating or cooling the reactor.

8 Acknowledgment

I want to thank the PCS group for the wonderful experience I could obtain. Thank you for the warm and welcomed atmosphere. Special thanks go to Alex and Kasper for their supportive nature. Furthermore, I would like to thank Prof. Dr. Guido Mul for taking the role as my supervisor and showing so much interest in my results. At last I want to thank Joana for her dedication in my thesis. Your guidance allowed me to learn a lot in such a short time and it was a pleasure working with you.

Should I ever work in a research group again, let's say for my master thesis, this group will have to compete with a very high level, YOURS!

Appendices

A | Absorption spectra

This part of the appendix contains the absorption spectra which were used to determine the concentration profile for degradation tests with the organic compounds and the variously platinum loaded catalyst.

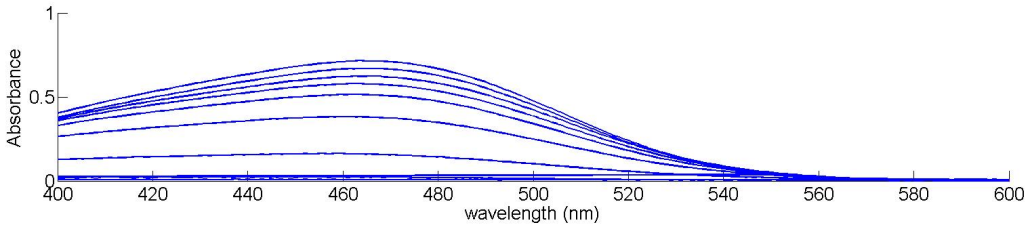

(a) Absorption spectrum of MO with TiO_2 P25 with photodeposition treatment

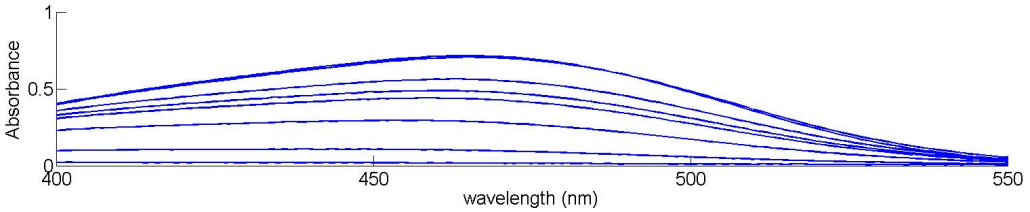

(b) Absorption spectrum of MO with 0.4 wt %Pt - P25

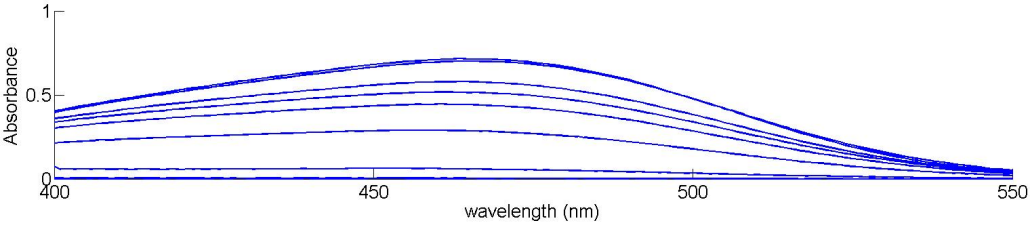

(c) Absorption spectrum of MO with 1 wt %Pt - P25

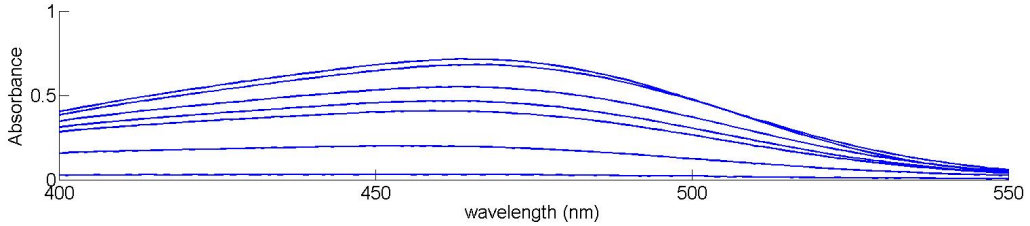

(d) Absorption spectrum of MO with TiO_2 P25 without photodeposition treatment

Figure A.1: Absorption spectra for MO and various catalyst samples

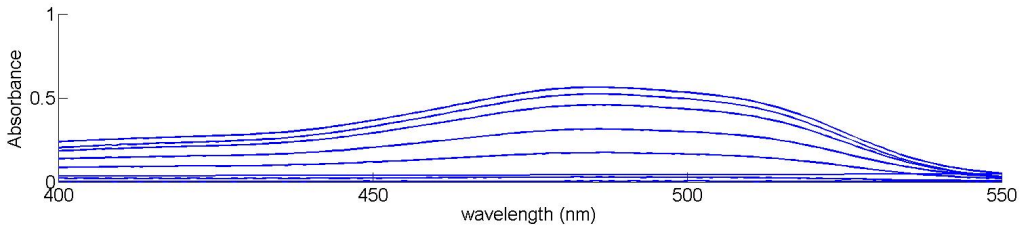

(a) Absorption spectrum of AO with TiO_2 P25 with photodeposition treatment

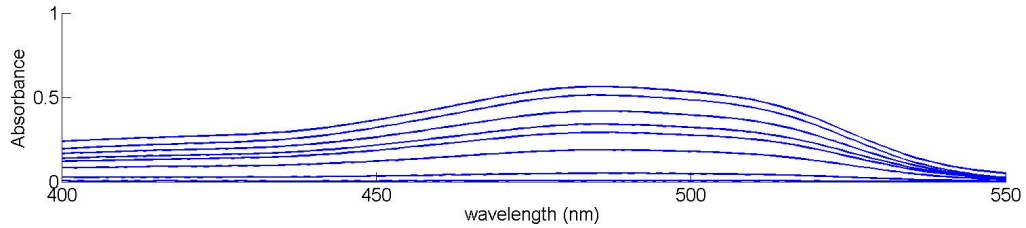

(b) Absorption spectrum of AO with 0.4 wt %Pt - P25

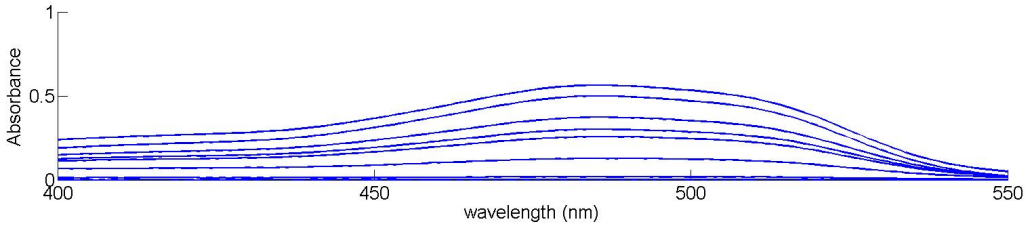

(c) Absorption spectrum of AO with 1 wt %Pt - P25

Figure A.2: Absorption spectra for AO and various catalyst samples

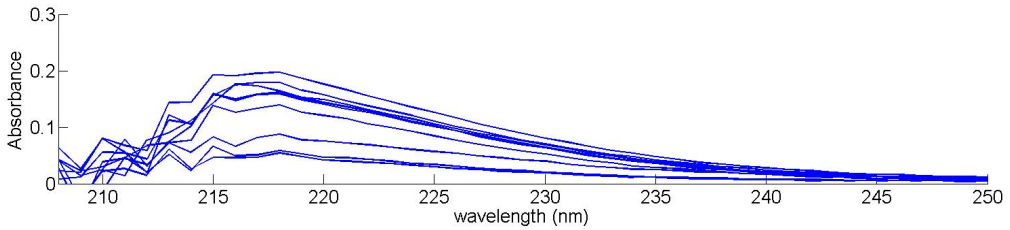

(a) Absorption spectrum of FA with TiO_2 P25 with photodeposition treatment

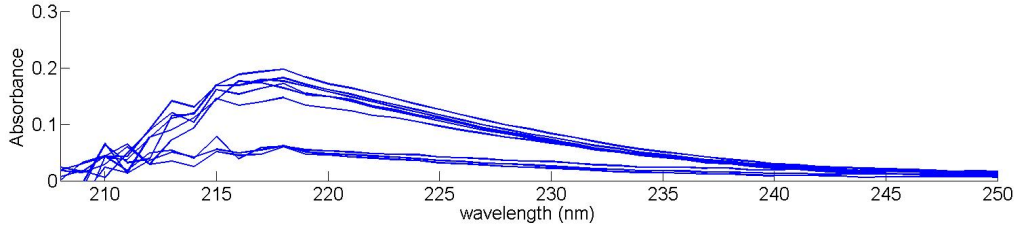

(b) Absorption spectrum of FA with 0.4 wt %Pt - P25

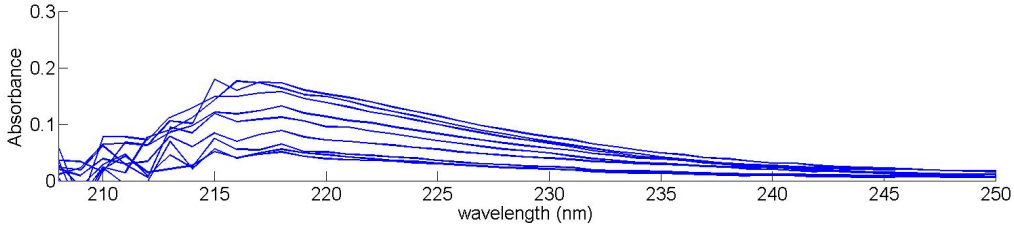

(c) Absorption spectrum of FA with 1 wt %Pt - P25

Figure A.3: Absorption spectra for FA and various catalyst samples

B Repeated degradation measurements

Some tests were performed twice. Those results are presented in this part of the appendix.

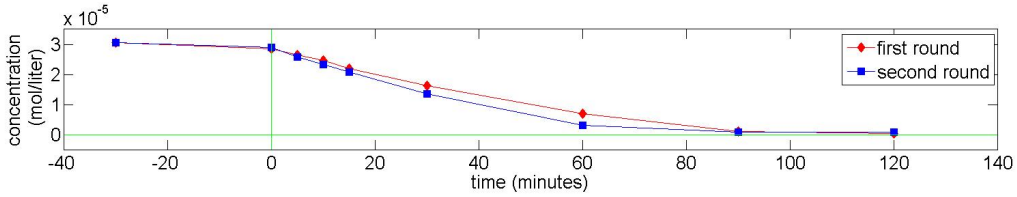

(a) repeated methyl orange degradation using non platinized TiO_2

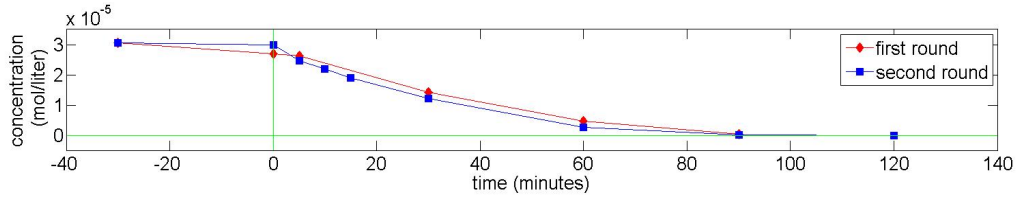

(b) repeated methyl orange degradation using 1 wt %Pt TiO_2

Figure B.1: Repeated methyl orange degradation tests

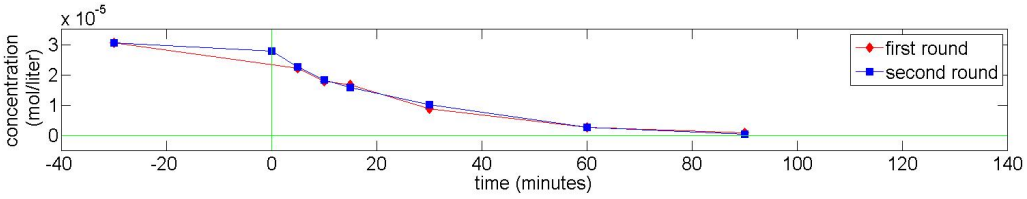

(a) repeated acid orange degradation using 0.4 wt %Pt TiO_2

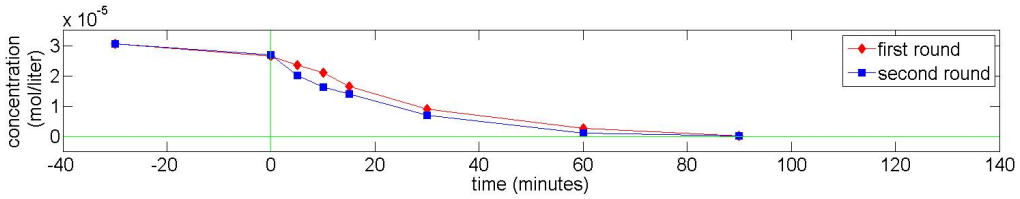

(b) repeated acid orange degradation using 1 wt %Pt TiO_2

Figure B.2: Repeated acid orange degradation tests

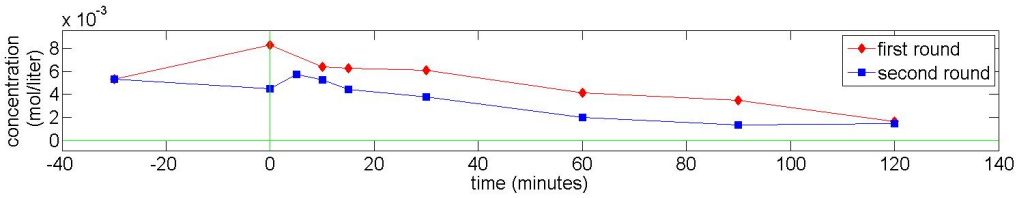

(a) repeated formic acid degradation using non platinized TiO_2

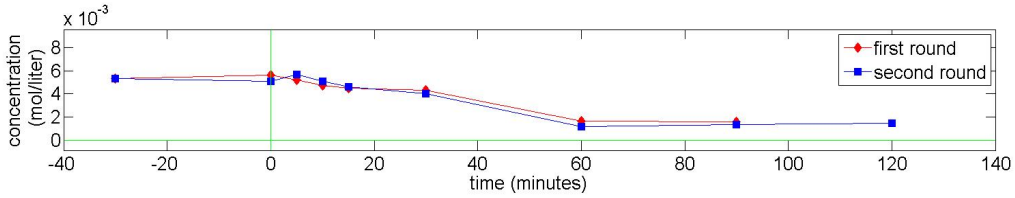

(b) repeated formic acid degradation using 0.4 wt %Pt TiO_2

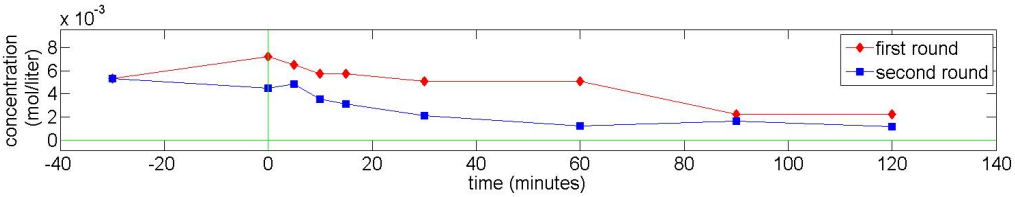

(c) repeated formic acid degradation using 1 wt %Pt TiO_2

Figure B.3: Repeated acid orange degradation tests

C Calibration line for hydrogen concentration determination

The signal detected by the TCD was transformed via a calibration curve to concentration values in ppm. The calibration curve is presented in Figure C.1

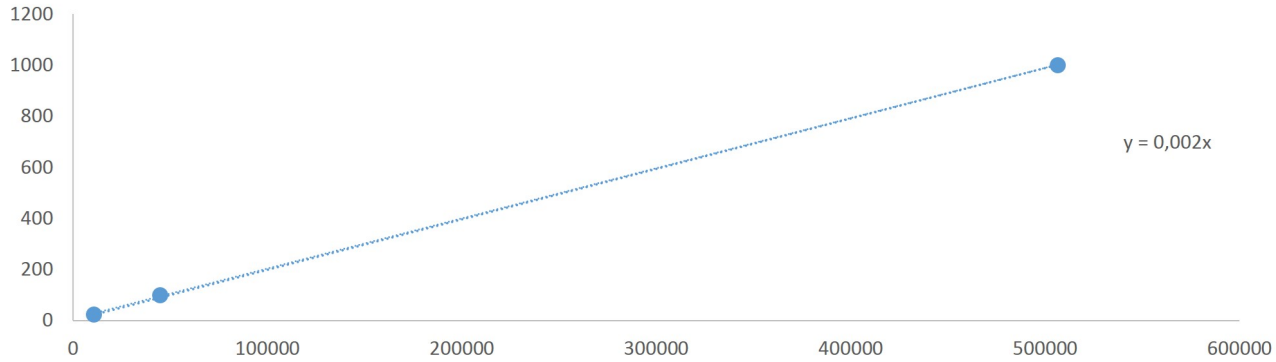

Figure C.1: Calibration curve for the determination of hydrogen concentrations

Bibliography

[1] Meng Ni, Michael K.H. Leung, Dennis Y.C. Leung, and K. Sumathy. A review and recent developments in photocatalytic water-splitting using for hydrogen production. *Renewable and Sustainable Energy Reviews*, 11(3):401 – 425, 2007.

[2] J-M Herrmann. Heterogeneous photocatalysis: state of the art and present applications in honor of pr. rl burwell jr.(1912–2003), former head of ipatieff laboratories, northwestern university, evanston (ill). *Topics in Catalysis*, 34(1-4):49–65, 2005.

[3] Michael R. Hoffmann, Scot T. Martin, Wonyong. Choi, and Detlef W. Bahnemann. Environmental applications of semiconductor photocatalysis. *Chemical Reviews*, 95(1):69–96, 1995.

[4] Saber Ahmed, M.G. Rasul, WaydeN. Martens, Richard Brown, and M.A. Hashib. Advances in heterogeneous photocatalytic degradation of phenols and dyes in wastewater: A review. *Water, Air, & Soil Pollution*, 215(1-4):3–29, 2011.

[5] Meng Nan Chong, Bo Jin, Christopher W.K. Chow, and Chris Saint. Recent developments in photocatalytic water treatment technology: A review. *Water Research*, 44(10):2997 – 3027, 2010.

[6] Yuexiang Li, Gongxuan Lu, and Shuben Li. Photocatalytic production of hydrogen in single component and mixture systems of electron donors and monitoring adsorption of donors by in situ infrared spectroscopy. *Chemosphere*, 52(5):843–850, 2003.

[7] F.B. Li and X.Z. Li. The enhancement of photodegradation efficiency using pt-tio2 catalyst. *Chemosphere*, 48(10):1103 – 1111, 2002.

[8] Alexia Patsoura, Dimitris I. Kondarides, and Xenophon E. Verykios. Enhancement of photoinduced hydrogen production from irradiated pt-tio2 suspensions with simultaneous degradation of azo-dyes. *Applied Catalysis B: Environmental*, 64(3-4):171 – 179, 2006.

[9] A. Mills and S.-K. Lee. Platinum group metals and their oxides in semiconductor photosensitisation. *Platinum Metals Review*, 47(1):2–12, 2003.

[10] Youji Li, Xiaodong Li, Junwen Li, and Jing Yin. Photocatalytic degradation of methyl orange by tio2-coated activated carbon and kinetic study. *Water Research*, 40(6):1119 – 1126, 2006.

[11] ShipraMital Gupta and Manoj Tripathi. A review of tio2 nanoparticles. *Chinese Science Bulletin*, 56(16):1639–1657, 2011.

[12] David O Scanlon, Charles W Dunnill, John Buckeridge, Stephen A Shevlin, Andrew J Logsdail, Scott M Woodley, C Richard A Catlow, Michael J Powell, Robert G Palgrave, Ivan P Parkin, et al. Band alignment of rutile and anatase tio2. *Nature materials*, 12(9):798–801, 2013.

[13] Yanqin Gai, Jingbo Li, Shu-Shen Li, Jian-Bai Xia, and Su-Huai Wei. Design of narrow-gap tio2: A passivated codoping approach for enhanced photoelectrochemical activity. *Phys. Rev. Lett.*, 102:036402, Jan 2009.

[14] Jungwon Kim, Chul Wee Lee, and Wonyong Choi. Platinized wo3 as an environmental photocatalyst that generates oh radicals under visible light. *Environmental Science & Technology*, 44(17):6849–6854, 2010.

[15] M. Nic, J. Jirat, B. Kosata, and A. Jenkins. Beer lambert law (or beer lambert bouguer law), 1997.

[16] E. Prichard, B. Stuart, and R.S. Chemistry. *Gas Chromatography*. Practical laboratory skills training guides. Royal Society of Chemistry, 2003.

[17] J. Sevcik. *DETECTORS IN GAS CHROMATOGRAPHY*. Journal of Chromatography Library. Elsevier Science, 2011.

[18] Kirk Snavely and Bala Subramaniam. Thermal conductivity detector analysis of hydrogen using helium carrier gas and hayesep d columns. *Journal of Chromatographic Science*, 36(4):191–196, 1998.

[19] M. Ermrich and D. Opper. *XRD for the Analyst: Getting Acquainted with the Principles*. PANalytical, 2013.

[20] ShipraMital Gupta and Manoj Tripathi. A review of tio2 nanoparticles. *Chinese Science Bulletin*, 56(16):1639–1657, 2011.

[21] Chieh-Chao. *Photocatalytic CO2 activation by water - catalyst screening and mechanistic evaluation*. PhD thesis, June.

[22] Kheamrutai Thamaphat, Pichet Limsuwan, and Boonlaer Ngotawornchai. Phase characterization of tio2 powder by xrd and tem. *Kasetsart J.(Nat. Sci.)*, 42(5):357–361, 2008.

[23] E. Pulido Melián, Cristina R. López, A. Ortega Méndez, O. González Díaz, M. Nereida Suárez, J.M. Do na Rodríguez, J.A. Navío, and D. Fernández Hevia. Hydrogen production using pt-loaded tio2 photocatalysts. *International Journal of Hydrogen Energy*, 38(27):11737 – 11748, 2013.

[24] Lung Chyuan Chen and Tse Chuan Chou. Kinetics of photodecolorization of methyl orange using titanium dioxide as catalyst. *Industrial & Engineering Chemistry Research*, 32(7):1520–1527, 1993.

[25] Luma M. Ahmed, Irina Ivanova, Falah H. Hussein, and Detlef W. Bahnemann. Role of platinum deposited on tio2 in photocatalytic methanol oxidation and dehydrogenation reactions. *International Journal of Photoenergy*, 2014, 2014.

[26] XZ Li and FB Li. Surface characterization and photocatalytic reactivity of innovative ti/tio2 and ti/pt-tio2 mesh photoelectrodes. *Journal of applied electrochemistry*, 32(2):203–210, 2002.

[27] Siham Al-Qaradawi and Salman R Salman. Photocatalytic degradation of methyl orange as a model compound. *Journal of Photochemistry and photobiology A: Chemistry*, 148(1):161–168, 2002.

[28] Pengfei Ji, Jinlong Zhang, Feng Chen, and Masakazu Anpo. Study of adsorption and degradation of acid orange 7 on the surface of ceo2 under visible light irradiation. *Applied Catalysis B: Environmental*, 85(3-4):148 – 154, 2009.

[29] Keon Woo Lee, Kyoung-Seok Lee, Kyung-Hoon Jung, and Hans-Robert Volpp. The 212.8-nm photodissociation of formic acid: Degenerate four-wave mixing spectroscopy of the nascent oh radicals. *The Journal of Chemical Physics*, 117(20), 2002.

[30] MC Hidalgo, M Maicu, and Nav. Photocatalytic properties of surface modified platinised tio2: effects of particle size and structural composition.

[31] Chun He, Ya Xiong, Xihai Zhu, and Xiangzhong Li. A platinised tio2 film with both photocatalytic and non-photocatalytic activities towards the oxidation of formic acid. *Applied Catalysis A: General*, 275(1-2):55 – 60, 2004.

[32] N Guettai and H Ait Amar. Photocatalytic oxidation of methyl orange in presence of titanium dioxide in aqueous suspension. part i: Parametric study. *Desalination*, 185(1):427–437, 2005.

[33] Wenjuan Li, Danzhen Li, Yangming Lin, Peixian Wang, Wei Chen, Xianzhi Fu, and Yu Shao. Evidence for the active species involved in the photodegradation process of methyl orange on tio2. *The Journal of Physical Chemistry C*, 116(5):3552–3560, 2012.

[34] HC Urey, LH Dawsey, and FO Rice. The absorption spectrum and decomposition of hydrogen peroxide by light. *Journal of the American Chemical Society*, 51(5):1371–1383, 1929.

[35] Najah Wehbe, Mira Jaafar, Chantal Guillard, Jean-Marie Herrmann, Sylvain Miachon, Eric Puzenat, and Nolven Guilhaume. Comparative study of photocatalytic and non-photocatalytic reduction of nitrates in water. *Applied Catalysis A: General*, 368(1-2):1 – 8, 2009.

[36] Anna Galinska and Jerzy Walendziewski. Photocatalytic water splitting over pt-tio2 in the presence of sacrificial reagents. *Energy & Fuels*, 19(3):1143–1147, 2005.

[37] Hyung-Joo Choi and Misook Kang. Hydrogen production from methanol/water decomposition in a liquid photosystem using the anatase structure of cu loaded. *International Journal of Hydrogen Energy*, 32(16):3841 – 3848, 2007. TMS06: Symposium on Materials in Clean Power Systems.

[38] S.-K. Lee and A. Mills. Platinum and palladium in semiconductor photocatalytic systems. *Platinum Metals Review*, 47(2):61–72, 2003.

[39] L. Gomathi Devi, S. Girish Kumar, K. Mohan Reddy, and C. Munikrishnappa. Photo degradation of methyl orange an azo dye by advanced fenton process using zero valent metallic iron: Influence of various reaction parameters and its degradation mechanism. *Journal of Hazardous Materials*, 164(2-3):459 – 467, 2009.